JCTC Journal of Chemical Theory and Computation

Article

pubs.acs.org/JCTC

Can Metallapyrimidines Be Aromatic? A Computational Study into a New Class of Metallacycles

Brian T. Psciuk, Richard L. Lord,*,† Charles H. Winter, and H. Bernhard Schlegel

Department of Chemistry, Wayne State University, Detroit, Michigan 48202, United States

Supporting Information

ABSTRACT: The aromaticity of a series of metallapyrimidines involving second row transition metals was examined using density functional theory. Nucleus independent chemical shifts (NICS) placed above the ring ($NICS(1)_{zz}$) were used to gauge the amount of aromaticity. Natural chemical shielding analysis (NCS) was employed to decompose the chemical shifts in terms of diamagnetic and paramagnetic contributions from individual molecular orbitals. While $NICS(1)_{zz}$ for niobapyrimidine, $[(pz)_2(Nb\text{-}pyr)]^0$, suggested slightly aromatic character, the NCS analysis shows this is due to the diamagnetic (field-free) contribution. Instead, the positive paramagnetic (field-induced) contribution suggests that niobapyrimidine may be slightly antiaromatic. A series of d^0 metallapyrimidines, $[(pz)_2(M\text{-}pyr)]$ with M = Y^{III}, Zr^{IV}, Nb^{V}, Mo^{VI}, Tc^{VII}, demonstrated similar behavior. Variation of the number of metal d electrons in a series of M^{V} metallapyrimidines, $[(pz)_2(M\text{-}pyr)]$ where M = Mo, Tc, Ru, and Rh, showed strong evidence for aromaticity, with $NICS(1)_{zz}$ values of −15.4, −36.0, −31.6, and −22.4, respectively, that are comparable to benzene (−28.7). NCS analysis of the Tc^{V}, Ru^{V}, and Rh^{V} complexes shows that aromaticity is favored by an unoccupied $d-\pi$ orbital that serves as an acceptor to facilitate conjugation in the metallapyrimidine ring. This unoccupied orbital is not sufficient as the d^0 series of complexes demonstrated, and we propose that the occupied $d-\delta$ orbital prevents bond localization and enables aromaticity in these metallacycles.

INTRODUCTION

Despite being introduced in the middle 1800s,[1] aromaticity is still a topical concept that fascinates experimental and theoretical chemists alike.[2] The bonding theories developed to explain benzene are a cornerstone of electronic structure theory. Aromaticity is so fundamental that introductory chemistry books present benzene and other $4n+2$ π systems as aromatic, while in reality there is no single, universally accepted measure of aromaticity. Some definitions of aromaticity are based on structural equivalences in the ring,[3] while others are based on the energetic stabilization of the cyclical form.[4] A comprehensive collection of definitions would span numerous volumes.[5] A commonly invoked set of consequences predicted by simple quantum mechanical models is summarized in Pople's ring-current model that was introduced to explain downfield proton shifts.[6] In this model, an applied magnetic field perpendicular to the ring of interest induces current in the conjugated π system, which in turn creates a magnetic field that opposes (aligns with) the applied field outside (inside) the ring. While this model was originally developed to explain proton resonances and has received criticism it its general application,[7] ring current is well-established and nonexperimentally observable quantities are readily computed.[8]

Aromatic systems where one of the CH groups is replaced by ML_n have attracted considerable attention in this field.[9] First investigated theoretically by Hoffmann,[10] these molecules have been intensely studied by a variety of computational methods over the past decade, with particular attention paid to their aromatic character.[11] Metal chelates are not typically aromatic,[12] but it is generally agreed upon that metallabenzenes are weakly aromatic. Questions still remain, such as how many of the d orbital electrons are involved in aromaticity[9a,10,11b,d] and what are the structural and electronic requirements for aromaticity in metallacycles. Our goal in the present paper is to explore the structure, bonding, and some magnetic criteria in a newly identified class of metallacycles, namely metallapyrimidines, that may shed some light on the larger question of aromaticity in metallacycles.

In this paper, we investigate a simplified example of our previously reported niobapyrimidine[13] and a series of hypothetical metallapyrimidine complexes containing second-row transition metals to provide a better understanding of the structure and bonding in this new class of metallacycle. First, we explore a putative mechanism for the formation of the previously isolated niobapyrimidine. Next, we use nucleus independent chemical shift (NICS)[8b] values to evaluate the aromaticity of niobapyrimidine and compare them to established aromatic and antiaromatic systems. NICS calculations can be misleading due to non-π orbital contributions, especially for inorganic systems;[14] so, we decompose the total chemical shift into orbital-specific components using the natural chemical shielding (NCS) analysis in NBO.[15] To understand how metal−ligand covalency affects aromaticity, we study a series of isoelectronic d^0 metallapyrimidines featuring second-row transition metals in a variety of oxidation states (Y^{III} through Tc^{VII}). Finally, we vary the d electron count of the metal by studying formally pentavalent metals in neutral metallapyrimidine complexes. The NCS analysis of each series

Special Issue: Berny Schlegel Festschrift

Received: August 7, 2012
Published: September 28, 2012

provides insight into how aromaticity might be encouraged in this new class of metallacycle.

COMPUTATIONAL DETAILS

All calculations were performed using a development version of Gaussian.[16] Geometry optimizations were carried out at the B3LYP/6-31G+(d) level of theory,[17] with metal atoms represented by the Stuttgart−Dresden−Bonn (SDD) effective core potential and its accompanying basis set.[18] Wave functions were tested for wave function stability,[19] and all optimized structures were confirmed as minima or transition states by analyzing the harmonic vibrational frequencies.[20] Transition states were obtained through full transition state searches and confirmed to connect reactant and product using an intrinsic reaction coordinate calculation.[21] For thermodynamic discussions, we analyzed both the electronic energy (E_{el}) and the gas-phase Gibbs free energy (G_g°). The gas-phase Gibbs free energy was obtained by adding to E_{el} the zero-point vibrational energy (ZPE) and the thermal free energy corrections ($\Delta G^\circ_{0\rightarrow 298K}$) derived from standard approximations (eq 1).[22]

$$G_g^\circ = E_{el} + \mathrm{ZPE} + \Delta G^\circ_{0\rightarrow 298K} \quad (1)$$

We used the nucleus independent chemical shift (NICS) method[8b,23] to evaluate aromaticity due to its conceptual simplicity and accessibility in standard quantum chemistry packages. NICS(0) is evaluated by placing a ghost atom (Bq) at the geometric mean of the ring atoms and computing the isotropic chemical shift (σ_{iso}) at this ghost atom. Due to sign convention, NICS(0) = $-\sigma(\mathrm{Bq})_{iso}$, we report $-\sigma$ values throughout the paper for consistency. Large negative values indicate aromaticity, while large positive values indicate antiaromaticity. Since the introduction of this aromaticity criterion, a number of improved NICS metrics have been proposed that overcome failures in NICS(0) such as for inorganic systems such as the ones we are studying.[14] For our work, we study the NICS$(1)_{zz}$ value that measures the chemical shift tensor component orthogonal to the ring at a point located 1 Å above the NICS(0) point. We evaluated NICS$(1)_{zz}$ both above and below the ring because there was not always a mirror plane containing the metallacycle. This was accomplished by constructing the normalized cross product between the NICS(0)−M and NICS(0)−N vectors. Chemical shift tensor components were evaluated using the Gauge-Including Atomic Orbital (GIAO) formalism.[24] Molecules were realigned so the three Bq atoms defined the z-axis, which allowed us to analyze the chemical shift tensor component orthogonal to the ring of interest (σ_{zz}). Finally, an orbital decomposition of NICS$(1)_{zz}$ was performed using the Natural Chemical Shielding (NCS) program in NBO.[15] NCS decomposes the total chemical shift into diamagnetic (field-free) and paramagnetic (field-induced) contributions from natural localized molecular orbitals and enabled us to analyze contributions to NICS$(1)_{zz}$ due only to π orbitals. All NBO calculations were performed using version 3.1 that is built in to Gaussian.[25]

RESULTS AND DISCUSSION

Niobapyrimidine Formation. We recently reported the unexpected formation and isolation of the first niobapyrimidine.[13] We were investigating metal complexes with multiple pyrazolate ligands as volatile precursors for atomic layer deposition film growth.[26] Use of Nb^{III}, Nb^{IV}, and Ta^{IV} salts led to isolation of the first niobapyrimidine, niobapyridinium, and tantalapyridinium complexes, respectively. We focus here on the simpler metallapyrimidine class that does not involve a protonated nitrogen. In the synthesis of the niobapyrimidine complex, a niobium(III) salt was reacted with a pyrazolate (pz) salt, and the expected product was $[Nb^{III}(pz)_3]^0$. Instead, we isolated the *bis*-pyrazolate niobapyrimidine complex shown in Scheme 1. Because we will refer to this compound and similar

Scheme 1. $[(pz)_2(Nb\text{-}pyr)]^0$

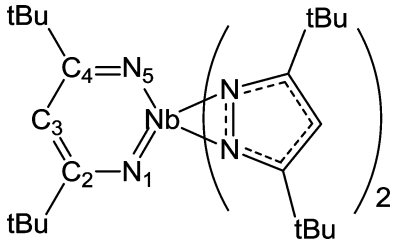

species throughout this manuscript, we introduce the shorthand $[(L)_2(M\text{-}pyr)]^{n+}$ to denote a *bis*-ligated metallapyrimidine. The structure in Scheme 1 is abbreviated $[(pz)_2(Nb\text{-}pyr)]^0$ in this notation.

The ring-opening activation of pyrazolates by metal complexes is rare, but not unprecedented.[27] The compounds of interest here are unique because they involve the activation of a pyrazolate N−N bond at a single metal center. In the case of $[(pz)_2(Nb\text{-}pyr)]^0$, the ring-opening oxidative addition of the N−N bond presumably occurs after formation of an intermediate *tris*-pyrazolate complex. To understand this transformation better, we investigated the electronic structure of the hypothetical $[Nb(pz)_3]^0$ species and the reaction path leading to $[(pz)_2(Nb\text{-}pyr)]^0$. This was done for a simplified system where the ^{t}Bu groups on C_2 and C_4 employed experimentally for steric protection and solubility were replaced with hydrogens.

Despite not being isolated and characterized experimentally, we were able to find a well-defined minimum for the $[Nb(pz)_3]^0$ complex. The optimized structure of $[Nb(pz)_3]^0$ is best described as a low-spin d^2-Nb^{III} species; the HOMO is a doubly occupied Nb d orbital that is more than 3.13 eV higher in energy than the HOMO-1 (pyrazolate-π), and only 2.32 eV lower in energy than the LUMO (another Nb d orbital). The complex is C_s symmetric (Figure 1, $[Nb(pz)_3]^0$), and all three of the pyrazolates are η^2 bound and have similar structures, as exemplified by the N−N bond lengths of 1.36 to 1.38 Å. This suggests the pyrazolates in this reactant are not activated, or at least that no one of the three is more predisposed to N−N cleavage than the others. We identified a C_1 symmetric transition state that involves rotation of the two nonactivated pyrazolates in opposite directions, and a significant amount of activation of the third pyrazolate (Figure 1, TS). This is evidenced by the N−N distance of 1.84 Å and Nb−N bond lengths of 1.93 and 2.06 Å. The pyrazolate is ∼40% activated in the transition state when compared to the final N−N separation of 2.61 Å in the product. The product (Figure 1, $[(pz)_2(Nb\text{-}pyr)]^0$ isomer 2) is C_s symmetric with the niobapyrimidine ring lying perpendicular to the mirror plane. The ring is slightly nonplanar with a ca. 10° deformation toward a chairlike structure. The Nb−N bond lengths are symmetric in the product with only a single value of 1.89 Å calculated. The ring C−C and C−N bonds are also symmetric and the pyrazolates are η^2 bound. The reaction barrier is

dx.doi.org/10.1021/ct3006979 | J. Chem. Theory Comput. 2012, 8, 4950−4959

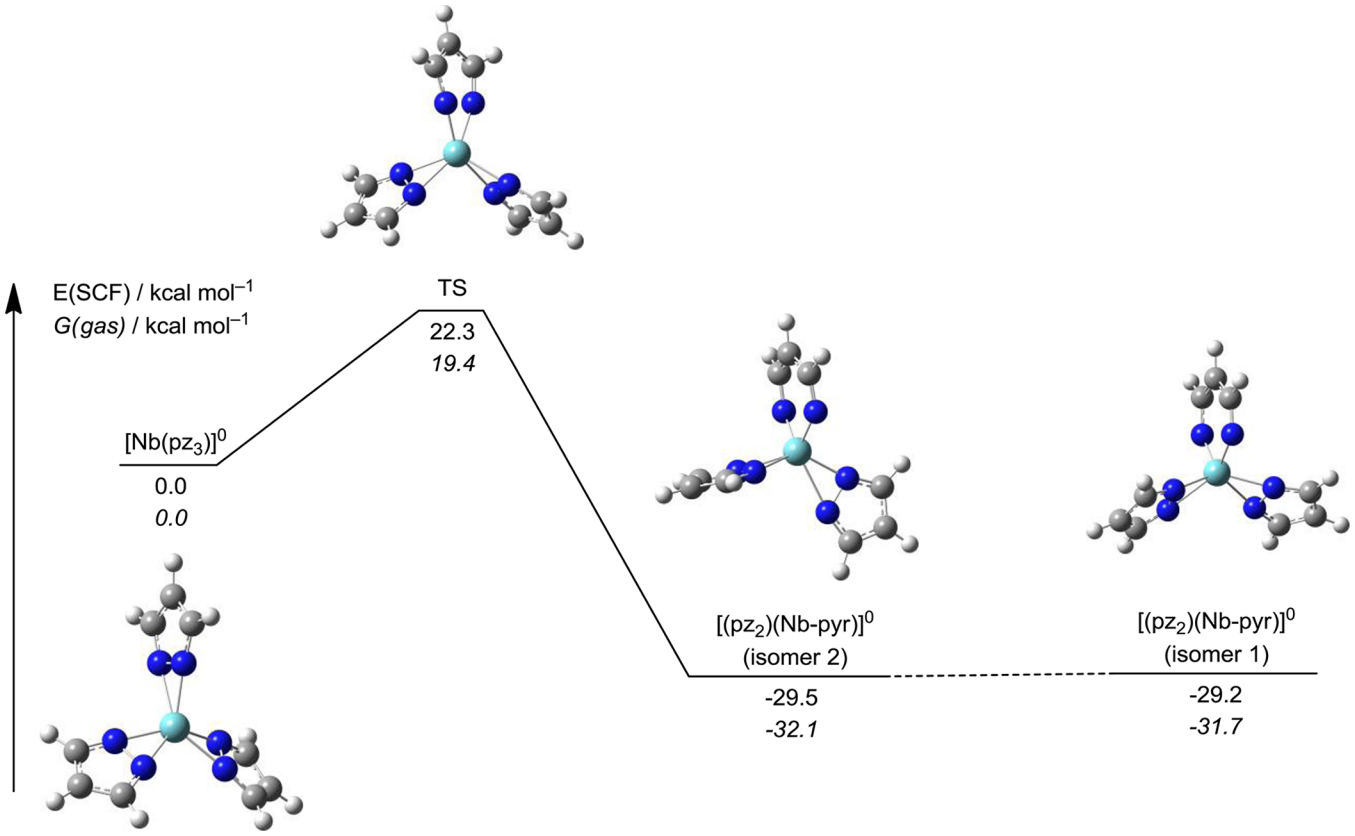

Figure 1. Potential energy surface and structures for the reaction of $[Nb(pz)_3]^0$ to form $[(pz)_2(Nb\text{-}pyr)]^0$.

consistent with facile activation at +22.3 kcal mol^{-1}, with a large driving force to product formation of −29.5 kcal mol^{-1}. We found an additional, isoenergetic isomer (+0.3 kcal mol^{-1}) of $[(pz)_2(Nb\text{-}pyr)]^0$ that is also C_s symmetric (isomer 1), but with a planar niobapyrimidine ring lying in the mirror plane. We expect the potential energy surface connecting isomer 1 and isomer 2 to be very flat based on low-frequency modes in both structures, and did not attempt to locate a transition state that connects isomer 1 to isomer 2 or to reactants. Isomer 1 showed asymmetry in the pyrimidine ring, as evidenced by Nb−N bond lengths of 1.83 and 1.98 Å, and was more similar in structure to the crystallographically determined structure with ^{t}Bu groups that also showed a nearly planar niobapyrimidine ring with bond asymmetry. It is possible that the bulky ^{t}Bu groups prevent isomer 2 from being accessible experimentally. While we present both species in Figure 1, we restrict our NICS analysis in the subsequent section to isomer 1, since it is more similar to existing experimental data and has a planar niobapyrimidine ring.

The major driving force for niobapyrimidine formation is the high energy Nb-based HOMO in the *tris*-pyrazolate complex. Oxidative addition of pyrazolate results in a d^0-Nb^V species that has a trianionic 3-ketimidoprop-1-en-1-imide (kp^{3-}, Scheme 2) ligand that forms the niobapyrimidine ring. The planarity of this ring raises a question about whether aromaticity may be another driving force for niobapyrimidine formation. In our previous report, NICS(1)$_{zz}$ calculations suggested that the niobapyrimidine ring was slightly aromatic, but there has been considerable concern in the literature about non-π contributions to the zz chemical shift tensor component used in NICS calculations, especially when metals are involved.[14a] Therefore, we investigated these results in further depth for $[(pz)_2(Nb\text{-}pyr)]^0$ and compared them to species for which the degree of aromaticity/antiaromaticity is well established: benzene, pyrimidine, cyclobutadiene, and the metallacycle rhodabenzene ($[(H_3P)_2(Cl)_2Rh(\kappa^2\text{-}C_5H_5)]^0$).

Scheme 2. Oxidative Fragment Interaction in $[(pz_2)(Nb\text{-}pyr)]^0$

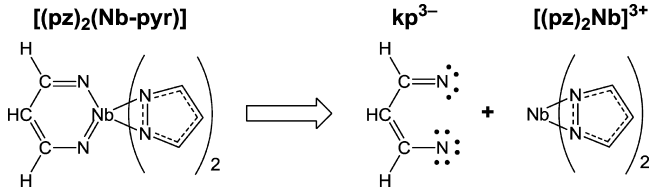

Natural Chemical Shielding for $[(pz)_2(Nb\text{-}pyr)]^0$. We previously computed NICS(1)$_{zz}$ values for the crystallographically determined structures of niobapyrimidine and niobapyridinium[13] (no optimization, full ^{t}Bu groups unlike the results presented here). On the basis of these results (NICS(1)$_{zz}$ = −9.9 and −5.5, respectively), we concluded that metallapyrimidines are weakly aromatic. The simplified model for niobapyrimidine studied here (^{t}Bu replaced by H) agrees well with a value of −8.8. Moreover, these values compare well to the NICS(1)$_{zz}$ value of −6.5 that we computed at the same level of theory for a related rhodabenzene species that has been established to be weakly aromatic.[11b,c] To put this in perspective, benzene and pyrimidine are computed to have NICS(1)$_{zz}$ values of −28.7 and −26.9, respectively, while cyclobutadiene has a value of +60.2. The NICS(1)$_{zz}$ metric was introduced to analyze the component of the chemical shift tensor perpendicular to the ring of interest. This should eliminate or greatly diminish contributions from orbitals not

dx.doi.org/10.1021/ct3006979 | J. Chem. Theory Comput. 2012, 8, 4950−4959

Table 1. Natural Chemical Shielding Analysis for Benzene, Pyrimidine, Cyclobutadiene, Rhodabenzene, and Niobapyrimidine[a]

species	NLMO description	total contribution	paramagnetic	diamagnetic
benzene $NICS(1)_{zz} = -28.7$	C−C π	−9.8	−5.6	−4.2
	C−C π	−9.8	−5.6	−4.2
	C−C π	−9.8	−5.6	−4.2
	$NICS(1)_{\pi zz}$	−29.4	−16.8	−12.6
pyrimidine $NICS(1)_{zz} = -26.9$	C−C π	−9.2	−4.9	−4.3
	C−N π	−9.1	−4.3	−4.8
	C−N π	−8.8	−4.4	−4.4
	$NICS(1)_{\pi zz}$	−27.1	−13.6	−13.5
cyclobutadiene $NICS(1)_{zz} = +60.2$	C−C π	27.3	30.7	−3.4
	C−C π	27.3	30.7	−3.4
	$NICS(1)_{\pi zz}$	54.6	61.4	−6.8
rhodabenzene $[(H_3P)_2(Cl)_2Rh(\kappa^2\text{-}C_5H_5)]^0$ $NICS(1)_{zz} = -6.5$	C−C−C π	−2.8	1.8	−4.6
	C−C−C π	−2.8	1.8	−4.6
	Rh d−π	−1.8	−2.0	0.2
	Rh d−δ	2.0	3.0	−1.0
	$NICS(1)_{\pi zz}$	−5.4	4.6	−10.0
niobapyrimidine $[(pz)_2(Nb\text{-}pyr)]^0$ $NICS(1)_{zz} = -8.8$	Nb−N π	−0.8	2.5	−3.3
	C−N π	−4.6	1.2	−5.8
	C−C π	−1.4	1.5	−2.9
	$NICS(1)_{\pi zz}$	−6.8	5.2	−12.0

[a] π orbital contributions (ppm) to the negative zz component of the chemical shielding tensor in the atomic origin for the ring of interest are listed.

involved with the π system, but we address this issue here explicitly by decomposing the $-\sigma_{zz}$ chemical shift tensor component into field-free (diamagnetic) and field-induced (paramagnetic) contributions from individual, localized molecular orbitals obtained through the Natural Chemical Shielding (NCS) analysis in NBO.[15] NCS results for the ring π orbitals are presented in Table 1 for benzene, pyrimidine, cyclobutadiene, rhodabenzene, and niobapyrimidine. Complete NCS tables with contributions from all orbital types (i.e., σ orbitals, π orbitals, etc.) may be found in the Supporting Information for all species, as well as isosurface plots for all π orbitals.

The sum of total contributions from π orbitals is formally equivalent to the $NICS(1)_{\pi zz}$ metric.[8b] To calibrate our expectations, we analyzed benzene, the classic example of an aromatic ring. The total contribution of the three π orbitals or $NICS(1)_{\pi zz}$ is −29.4 ppm, in good agreement with the $NICS(1)_{zz}$ value of −28.7 for benzene. While individual contributions from non-π orbitals are not zero, their sum is small, as evidenced by the small difference of 0.4 ppm. Each of the localized C−C π orbitals contributes −9.8 ppm to the overall sum with a paramagnetic contribution of −5.6 ppm and a diamagnetic contribution of −4.2 ppm. Similar results are found for pyrimidine, where the $NICS(1)_{\pi zz}$ of −27.2 ppm agrees well with the $NICS(1)_{zz}$ value of −26.9, with each of the three π orbitals contributing ∼−9 ppm. The C−N π orbitals of pyrimidine are slightly different from one another because one involves the carbon atom between the nitrogen atoms in the localized Lewis description of this π manifold. The C−C π orbital has a slightly larger paramagnetic and slightly smaller diamagnetic contribution than the C−N π orbitals, but all three make negative contributions similar to benzene. Cyclobutadiene provides a clear counterexample of antiaromaticity with a $NICS(1)_{zz}$ value of +60.2 that agrees with the $NICS(1)_{\pi zz}$ of 54.6 ppm, though there is a disagreement of ∼5 ppm that indicates other orbitals contribute to the NICS value. Each π orbital induces a large positive paramagnetic contribution of 30.7 ppm compared to the small negative diamagnetic contribution of −3.4 ppm. Thus, an indicator of highly aromatic (antiaromatic) systems is that the π orbitals make large negative (positive) paramagnetic contributions to the perpendicular chemical shift tensor used for the $NICS(1)_{zz}$ metric, consistent with the expectation of field-induced (paramagnetic) behavior.

Previous reports have established that rhodabenzene is weakly aromatic through energy decomposition analysis of the π bonding[11b] and induced current analysis.[11c] Therefore, we analyze that metallacycle species first. The $NICS(1)_{\pi zz}$ of −5.4 ppm agrees well with the $NICS(1)_{zz}$ value of −6.5, though this arises predominantly from diamagnetic (−10.0 ppm) and not paramagnetic (4.6 ppm) contributions. The total contribution of the Rh d orbitals is negligible (0.2 ppm), with the orbital pointing into the ring (d−π) making a small negative contribution (−1.8 ppm) and the orbital perpendicular to the ring (d−δ) making a small positive contribution (2.0 ppm). This is due to the paramagnetic contributions of −2.0 and 3.0 ppm, respectively. The two ring-based π orbitals contribute −2.8 ppm each. The value of −2.8 ppm is due to diamagnetic contributions (−4.6 ppm) with a small positive paramagnetic contribution (1.8 ppm). Niobapyrimidine, with a d^0-Nb^V center, has 6 π electrons. The $NICS(1)_{\pi zz}$ of −6.8 ppm agrees with the $NICS(1)_{zz}$ value of −8.8. Thus, one important point is that neither of the metallacycle $NICS(1)_{zz}$ values is qualitatively incorrect due to non-π contributions. The NBO analysis identified Nb−N, C−N, and C−C π bonds, consistent with the localization of bonds in the ring. The Nb−N bond contributes little (−0.8 ppm) compared to the C−N (−4.6 ppm) and C−C (−1.4 ppm) π bonds. This is similar to rhodabenzene, though in this case the orbital involving Nb makes a small negative

dx.doi.org/10.1021/ct3006979 | J. Chem. Theory Comput. 2012, 8, 4950−4959

rather than positive contribution. In both cases the slight aromatic character indicated by the NICS(1)$_{zz}$ value is due to negative diamagnetic contributions from the π bonds located on the organic fragment of the metallacycle. The finding of positive field-induced (paramagnetic) contributions and an overall negative chemical shift due to field-free (diamagnetic) contributions suggests that aromaticity may not be a strong driving force in these systems. This is consistent with our locating a second, isoenergetic structure (isomer 2) that has a nonplanar metallacycle, which would not be expected for an aromatic system.

d^0 [(pz)$_2$(M^{n+}-pyr)]$^{(n-5)+}$ Complexes (M = Y^{III}, Zr^{IV}, Nb^{V}, Mo^{VI}, Tc^{VIII}). We hypothesized that the ability of the formally trianionic kp^{3-} ligand to bond covalently with the d^0 metal is a critical feature in these metallacycles and thus for the potential aromaticity of the ring. Considering the metallacycle as an interaction of a *bis*-pyrazolate metal fragment and the trianionic kp^{3-} ligand fragment (see Scheme 2), the d^0 (pz)$_2$M fragment has two unoccupied d orbitals that can potentially accept electron density, and the kp^{3-} ligand has three occupied π orbitals (Figure 2). Of the two metal orbitals, the one pointing into the ring ($d-\pi$) is expected to be a stronger acceptor than the orbital perpendicular to the ring ($d-\delta$).

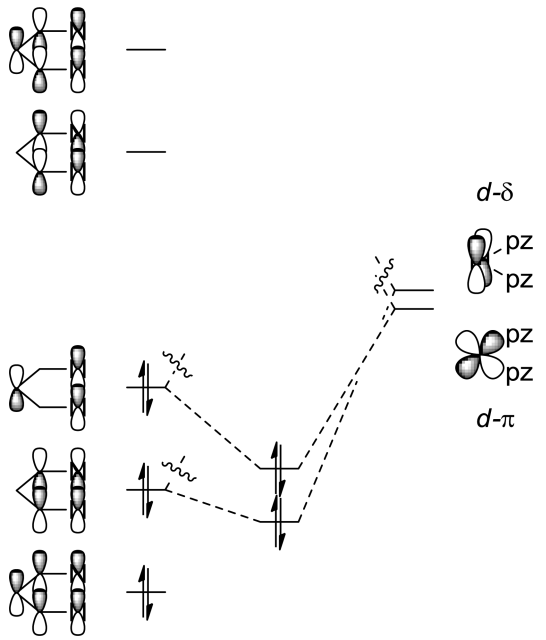

Figure 2. Simplified orbital interaction diagram between kp^{3-} (left) and (pz)$_2$M (right).

To explore the effect of metal oxidation state while maintaining a formal d-electron count of zero, we optimized a series of second-row transition metal complexes: [(pz)$_2$(Y^{III}-pyr)]$^{2-}$, [(pz)$_2$(Zr^{IV}-pyr)]$^{1-}$, [(pz)$_2$(Nb^{V}-pyr)]^{0}, [(pz)$_2$(Mo^{VI}-pyr)^{VI}]$^{1+}$, and [(pz)$_2$(Tc^{VII}-pyr)]$^{2+}$. We identified two structures for each of these species. One structure was similar to isomer 1 with bond length asymmetry in a planar metallapyrimidine ring, and the other structure was similar to isomer 2 with nearly symmetric bonds but a nonplanar metallapyrimidine ring. The Tc^{VII} complexes were the only exception, where we located a low symmetry structure that was intermediate between isomer 1 and isomer 2. This species was more stable than isomer 1 by 4.5 kcal mol^{-1}. This is in contrast to the other four complexes where isomer 1 and isomer 2 are isoenergetic. We label the lower energy structure for Tc^{VII} isomer 2 for convenience because the technetiapyrimidine ring is nonplanar. Bond lengths are presented in Table 2 for isomer 1 for each metal as well as isomer 2 for Tc^{VII}. We again choose to focus on isomer 1 because of its relevance to the established crystal structure and the planarity of the metallacycle. Cartesian coordinates for each isomer of all complexes investigated can be found in the Supporting Information.

The Y^{III} complex stands out in this series with η^1 pyrazolate ligands, while all of the other complexes have η^2 bound pyrazolates. Within the metallapyrimidine ring, the Y−N bonds are long (>2.1 Å) and similar to one another (Δ = 0.02 Å). The C−N and C−C bond lengths are very uniform at 1.308 ± 0.004 and 1.432 ± 0.004 Å, respectively. In contrast, the Nb−N bond lengths differ by 0.15 at 1.833 and 1.979 Å and are indicative of a localized bonding pattern consistent with the metallacycle shown in Scheme 1. The Zr^{IV} results are intermediate with some localization as evidenced by the difference in Zr−N bond lengths of 0.09 Å. Asymmetry in the M−N bonds is a maximum for Mo^{VI} with a difference of 0.16 Å, though this is very similar to the value for both Nb^{V} and Tc^{VII}. The Tc−N bonds for isomer 1 are both very short (<1.9 Å) but show an asymmetry of Δ = 0.15 Å. Isomer 2 for Tc^{VII} shows similar bonding, though the metal-pyrazolate bonding is slightly less asymmetric and less localized bonding in the ring is observed. There is a clear trend between the M−N bond lengths and metal oxidation state, but localization does not strictly increase with increasing oxidation state. Collectively, these trends suggest that our hypothesis of weaker metal−ligand communication with low metal oxidation states is correct. However, the Y^{III} species is the closest to having symmetric bonding within the metallacycle, which is usually argued as a criterion for aromaticity. Could less covalent bonding with the metal actually enhance aromaticity? We turned to the NCS analysis of the NICS(1)$_{zz}$ values to investigate this point further.

NICS(1)$_{zz}$ values range from +5.1 for Y^{III} to −19.7 for Tc^{VII} (isomer 1 only) where values follow an approximately linear trend with the metal oxidation state (Table 3). In each of these species, the NCS analysis of π orbital contributions is close to the NICS(1)$_{zz}$ value, suggesting the trend is not an artifact, but the contribution of non-π orbitals increases with metal oxidation state. For the Y^{III} complex none of the π orbitals have metal character (Figure 3). Combined with the NICS(1)$_{zz}$ value of +5.1 due to a large paramagnetic π contribution of 12.6 ppm, these results suggest that the Y complex is slightly antiaromatic and that the delocalized bond length pattern is not indicative of aromaticity. The Zr^{IV} C−N π orbitals show a slight amount of metal character, but the qualitative pattern is more similar to those of Y than those of the other complexes. For both Y and Zr the C−C−C π bond makes a large, positive paramagnetic contribution to the NICS(1)$_{\pi zz}$. The Nb, Mo, and Tc complexes were observed to have localized bonds consistent with the bond lengths in Table 2, and this is reflected in the orbital plots in Figure 3. Here, we observe a qualitatively different orbital pattern with localized M−N, C−N, and C−C π bonds. All three of these π bonds make an overall negative contribution of −1 to −6 ppm, but this is due to diamagnetic and not paramagnetic contributions. Although the Tc−N bond makes a negative paramagnetic contribution of −1.1 ppm, the paramagnetic π sum for the Tc^{VII} species is still 0.5 ppm. Overall paramagnetic contributions tend toward zero from 12.6

dx.doi.org/10.1021/ct3006979 | J. Chem. Theory Comput. 2012, 8, 4950−4959

Table 2. Metal-Pyrazolate and Metallapyrimidine Bond Lengths (Å) for the d^0 Series of Complexes

complex	M—pz	M═N_1	N_1—C_2	C_2═C_3	C_3—C_4	C_4═N_5	N_5—M
$[(\eta^1\text{-pz})_2(Y^{III}\text{-pyr})]^{2-}$	2.446	2.151	1.311	1.428	1.436	1.304	2.169
	3.325						
$[(\eta^2\text{-pz})_2(Zr^{IV}\text{-pyr})]^{1-}$	2.265	1.967	1.329	1.401	1.434	1.304	2.056
	2.389						
$[(\eta^2\text{-pz})_2(Nb^{V}\text{-pyr})]^{0}$	2.135	1.833	1.351	1.379	1.441	1.299	1.979
	2.223						
$[(\eta^2\text{-pz})_2(Mo^{VI}\text{-pyr})]^{1+}$	2.049	1.764	1.359	1.372	1.446	1.298	1.925
	2.122						
$[(\eta^2\text{-pz})_2(Tc^{VII}\text{-pyr})]^{2+}$ isomer 1	2.002	1.745	1.344	1.382	1.444	1.300	1.899
	2.068						
$[(\eta^2\text{-pz})_2(Tc^{VII}\text{-pyr})]^{2+}$ isomer 2	1.938/2.019	1.757	1.334	1.395	1.431	1.312	1.851
	2.292/2.089						

Table 3. Natural Chemical Shielding Analysis for the d^0 Series of $[(pz)_2(M^{n+}\text{-pyr})]^{(n-5)+}$ Complexes[a]

species	NLMO description	total contribution	paramagnetic	diamagnetic
Y^{III}	C−N π	−2.2	2.0	−4.3
$NICS(1)_{zz}$ = +5.1	C−N π	−1.5	2.9	−4.4
	C−C−C π	8.6	7.7	1.0
	$NICS(1)_{\pi zz}$	5.0	12.6	−7.7
Zr^{IV}	C−N π	−2.6	2.7	−5.4
$NICS(1)_{zz}$ = −3.0	C−N π	−5.9	−0.8	−5.1
	C−C−C π	5.7	5.1	0.6
	$NICS(1)_{\pi zz}$	−2.8	7.0	−9.8
Nb^{V}	Nb−N π	−0.8	2.5	−3.3
$NICS(1)_{zz}$ = −8.8	C−N π	−4.6	1.2	−5.8
	C−C π	−1.4	1.5	−2.9
	$NICS(1)_{\pi zz}$	−6.8	5.2	−12.0
Mo^{VI}	Mo−N π	−3.6	0.3	−3.9
$NICS(1)_{zz}$ = −14.1	C−N π	−4.9	1.7	−6.6
	C−C π	−1.9	1.7	−3.6
	$NICS(1)_{\pi zz}$	−10.3	3.7	−14.0
Tc^{VII}	Tc−N π	−4.9	−1.1	−3.8
$NICS(1)_{zz}$ = −19.7	C−N π	−5.7	1.1	−6.8
	C−C π	−3.4	0.6	−3.9
	$NICS(1)_{\pi zz}$	−14.0	0.5	−14.5

[a] π orbital contributions (ppm) to the negative zz component of the chemical shielding tensor in the atomic origin for the ring of interest are listed.

for Y^{III} to 0.5 for Tc^{VII} changing almost linearly with the oxidation state of the metal.

$NICS(1)_{zz}$ values suggest these d^0 complexes are weakly aromatic, while the field-induced (paramagnetic) contributions of the π orbitals and the isoenergetic, nonplanar isomers suggest instead that these compounds are non- or antiaromatic. Regardless of which metric we base our final conclusion on, the isoelectronic d^0 metallapyrimidines show no convincing patterns of aromaticity. The trend toward nonaromatic behavior with increasing oxidation state coincides with an increased amount of metal *d*-orbital character in the π orbitals. In an extreme limit, this would involve formal electron transfer from kp^{3-} to the metal. Therefore, this suggested to us that looking at isostructural metal complexes with different *d* electron counts, especially in the $d-\pi$ or $d-\delta$ orbital (Figure 2), could produce an aromatic metallapyrimidine.

M^V $[(pz)_2(M\text{-pyr})]^0$ Complexes (M = Nb^V, Mo^V, Tc^V, Ru^V, Rh^V). We turned our attention to a series of metallapyrimidines with formally pentavalent metals to evaluate the impact of *d* orbital occupation on the aromaticity of the metallacycle. Geometry optimization afforded a C_2 symmetric structure (C_2 axis along M−C_3) for all of the complexes except Nb^V (Figure 4). There is a noticeable deviation from a tetrahedral disposition as evidenced by N_{pz}−M−N_{pz} angles of 120−145 degrees. A structure similar to isomer 1 was also located on the potential energy surface for each of these pentavalent metal complexes, but isomer 1 is higher in energy than the C_2 symmetric structure by 8−12 kcal mol^{-1}. We also attempted to find a C_2 symmetric structure for Nb^V, but each attempted optimization reverted to isomer 2. The structural parameters for the C_2 symmetry structures of Mo^V thru Rh^V are included in Table 4. The most notable feature is that the M−N, C−N, and C−C bonds are equivalent in these metallacycles and, unlike the d^0 isomer 2 series that also featured equivalent bonds, each metallapyrimidine ring is planar. Short M−N bond lengths of 1.78−1.88 Å are observed in the metallapyrimidine ring, and

dx.doi.org/10.1021/ct3006979 | J. Chem. Theory Comput. 2012, 8, 4950−4959

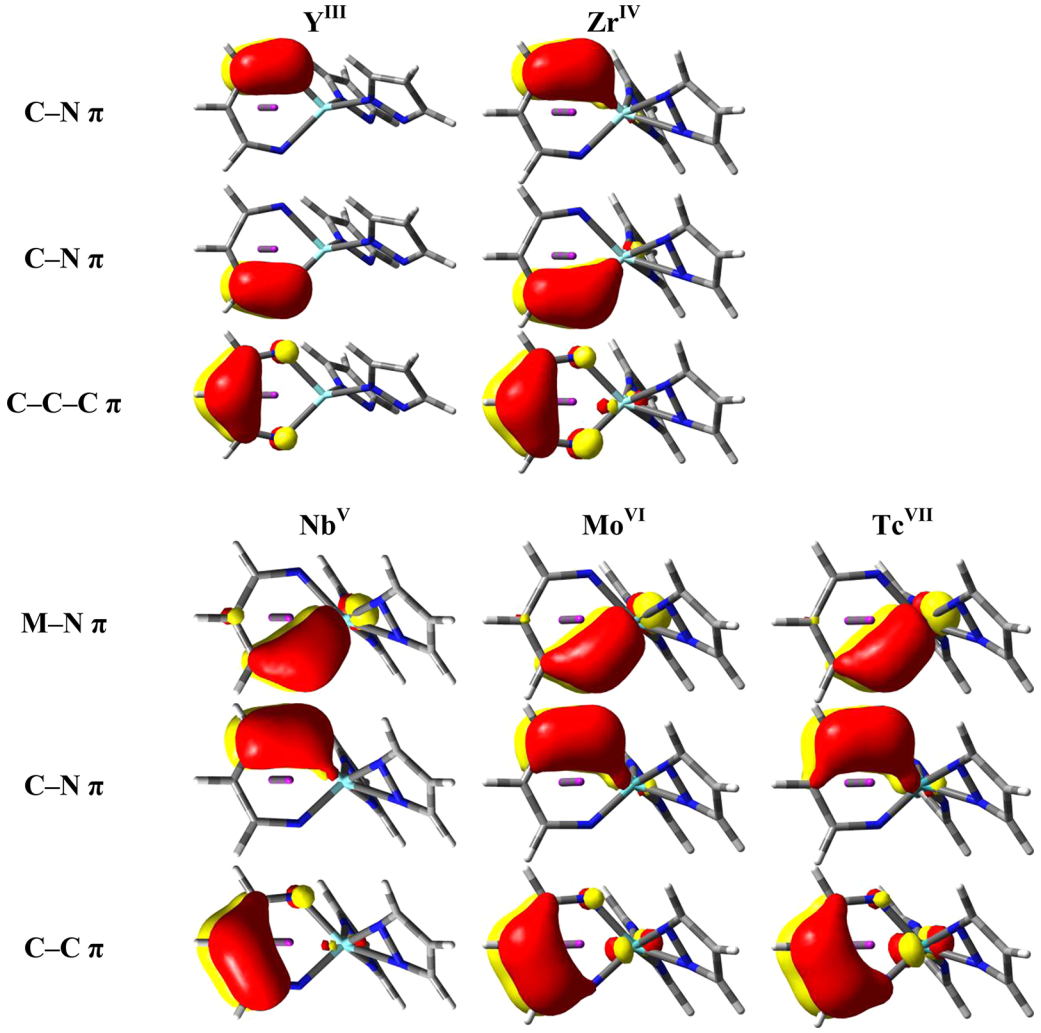

Figure 3. Molecular orbital isosurface plots (0.05 au) of the π orbitals for the $[(pz)_2(M^{n+}\text{-pyr})]^{(n-5)+}$ complexes.

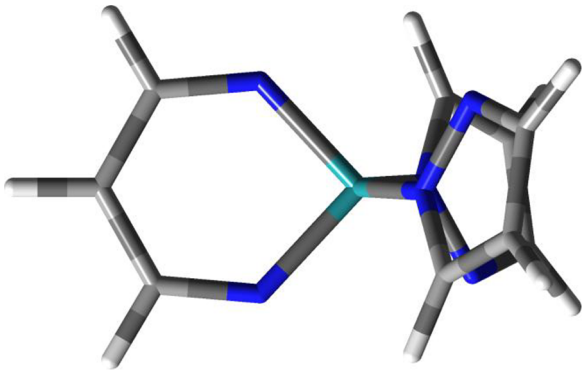

Figure 4. C_2 symmetric structure for the $[(pz)_2(M^{V}\text{-pyr})]^0$ complexes.

the C–N and C–C bond lengths varied between 1.31 and 1.33 and 1.40–1.41 Å, respectively. At the same level of theory, the C–N and C–C bond lengths for pyrimidine are 1.34 and 1.39 Å, respectively. The symmetric, planar geometry and the bond length data, combined with the fact that the localized isomer 1 structure is much higher in energy, suggest that these complexes demonstrate aromaticity.

To quantify the aromaticity in these complexes, we turned to the NICS/NCS analyses. $NICS(1)_{zz}$ values of −15.4, −36.0, −31.6, and −22.4 for the Mo^V, Tc^V, Ru^V, and Rh^V complexes further suggest that they are aromatic. In fact, these values compare well to the values of −28.7 and −26.9 for benzene and pyrimidine. However, the Tc^{VII} species in the d^0 complexes also had a reasonable $NICS(1)_{zz}$ value of −19.7 that, upon further investigation, was found to be due to diamagnetic and not paramagnetic contributions. The NCS breakdown is detailed for $[(pz)_2(Tc^V\text{-pyr})]^0$ and $[(pz)_2(Rh^V\text{-pyr})]^0$ in Table 5.

The $NICS(1)_{\pi zz}$ for the Tc^V species of −30.3 ppm agrees reasonably well with the $NICS(1)_{zz}$ value of −36.0. This value is due to a large negative paramagnetic contribution of −19.6 ppm and a diamagnetic contribution of −10.7 ppm, similar to the values of −16.6 and −12.7 ppm observed for benzene. Each of the ring π orbitals contributes between −8 and −9 ppm. The two C–N π orbitals have equal paramagnetic (−4.3 ppm) and diamagnetic (−4.8 ppm) contributions, while the deloc π orbital (see Figure 5) value is due entirely to paramagnetic contributions (−7.8 ppm). The Tc d–δ orbital also makes a negative contribution of −4.1 ppm that is predominantly due to paramagnetic contributions (−3.1 ppm). It is important to note that two of the Tc orbitals have the proper symmetry to conjugate with the ring: (i) the d–π orbital acts as an acceptor as evidenced in the orbital plot for the deloc π orbital (Figure 5), and (ii) the d–δ orbital acts as a weak donor. Thus, whether we consider it to be a 6-electron (excluding d–δ) or an 8-electron system that defies traditional electron counting for

dx.doi.org/10.1021/ct3006979 | J. Chem. Theory Comput. 2012, 8, 4950–4959

Table 4. Metal-Pyrazolate and Metallapyrimidine Bond Lengths (Å) for the M^V series of Complexes

complex	d electron count	S	M−pz	M−N	N−C	C−C
$[(\eta^1\text{-pz})_2(Mo^V\text{-pyr})]^0$	d^1	1/2	2.043	1.820	1.336	1.404
			2.499			
$[(\eta^1\text{-pz})_2(Tc^V\text{-pyr})]^0$	d^2	0	1.980	1.784	1.330	1.403
			2.856			
$[(\eta^1\text{-pz})_2(Ru^V\text{-pyr})]^0$	d^3	1/2	1.960	1.824	1.321	1.404
			2.843			
$[(\eta^1\text{-pz})_2(Rh^V\text{-pyr})]^0$	d^4	0	1.965	1.880	1.312	1.411
			2.830			

Table 5. Natural Chemical Shielding Analysis for the $[(pz)_2(M^V\text{-pyr})]^0$ Series of Complexes[a]

species	NLMO description	total contribution	paramagnetic	diamagnetic
Mo^V $NICS(1)_{zz} = -15.4$	C−N π	−4.3	0.1	−4.3
	C−N π	−4.3	0.1	−4.3
	deloc π	−1.8	1.2	−2.9
	Mo d−δ	−3.7	−1.4	−2.4
	$NICS(1)_{\pi zz}$	−14.1	−0.1	−14.0
Tc^V $NICS(1)_{zz} = -36.0$	C−N π	−9.2	−4.3	−4.8
	C−N π	−9.2	−4.3	−4.8
	deloc π	−7.8	−7.8	−0.1
	Tc d−δ	−4.1	−3.1	−1.0
	$NICS(1)_{\pi zz}$	−30.3	−19.6	−10.7
Ru^V $NICS(1)_{zz} = -31.6$	C−N π	−8.6	−4.3	−4.2
	C−N π	−8.6	−4.3	−4.2
	deloc π	−2.6	−2.1	−0.5
	Ru d−δ	−3.3	−2.6	−0.7
	$NICS(1)_{\pi zz}$	−23.0	−13.3	−9.7
Rh^V $NICS(1)_{zz} = -22.4$	C−N π	−7.1	−2.2	−4.9
	C−N π	−7.1	−2.2	−4.9
	deloc π	−4.6	−5.5	0.9
	Rh d−δ	−1.3	−0.6	−0.7
	$NICS(1)_{\pi zz}$	−20.0	−10.4	−9.6

[a] π orbital contributions (ppm) to the negative zz component of the chemical shielding tensor in the atomic origin for the ring of interest are listed. The C−N π-orbital chemical shift values have been averaged to reflect the symmetry in the molecule.

aromatic systems, the Tc^V complex provides a convincing example of aromaticity in a metallapyrimidine.

Despite seeming to be a 10-electron π system, the Rh^V complex shows similar behavior to that of technetium. This is misleading, however, as the coordination environment at the Rh center has the Rh d−δ orbital doubly occupied and another d orbital (nonbonding, in the plane of the metallacycle) that is orthogonal to the rhodapyrimidine π orbitals. Occupation of d−π is unfavorable because the orbital lobes partially overlap with the ancillary pyrazolate lone pairs, imparting antibonding character. Thus, the ring π electron count is still 8-electrons, and only four contributing orbitals are included in Table 5. The $NICS(1)_{\pi zz}$ of −20.0 ppm agrees well with the $NICS(1)_{zz}$ value of −22.4, which is smaller than that of the Tc^V complex but still indicative of strong aromaticity. Importantly, the paramagnetic contribution is greater than the diamagnetic contribution at −10.4 vs −9.6 ppm. The d−δ orbital has a small contribution of −1.3 here compared to −4.1 for Tc. All three of the π orbitals in the ring make negative contributions of −5 to −7 ppm. The deloc π orbital is dominated by the paramagnetic contribution of −5.5 ppm, with a positive diamagnetic contribution of 0.9 ppm. The C−N π orbitals make contributions of −7.1 ppm but this is mostly due to diamagnetic (−4.9 ppm) instead of paramagnetic (−2.2 ppm) contributions. We suspect this has to do with enlargement of the ring, most noticeable in the longer M−N bond lengths of 1.9 vs 1.8 Å for Rh^V vs Tc^V, due to occupation of the d-orbital that lies in the plane of the rhodapyrimidine.

Finally, we wanted to investigate whether metallapyrimidine formation is thermodynamically feasible for these species that demonstrate properties that are consistent with aromatic systems. While it does not prove that such compounds can be isolated in the lab, we evaluated the thermodynamics for $M^{III}(pz)_3 \rightarrow (pz)_2(M^V\text{-pyr})$ for each these species to see if ring-opening of the pyrazolate is feasible. Formation of the metallapyrimidine is exergonic by −29, −44, −48, and −24 kcal mol^{-1} for Nb, Mo, Tc, and Ru, but endergonic by 5 kcal mol^{-1} for Rh. This trend is sensible because both Ru^{III} and Rh^{III} are stable redox states for those metals and because the aromaticity is predicted to be largest for the Tc species providing a larger driving force for metallacycle formation. Such low coordination number complexes of Mo and Tc are unlikely to be isolated without the use of extremely bulky steric groups on the pyrazolates, but we are working to find feasible redox

dx.doi.org/10.1021/ct3006979 | J. Chem. Theory Comput. 2012, 8, 4950−4959

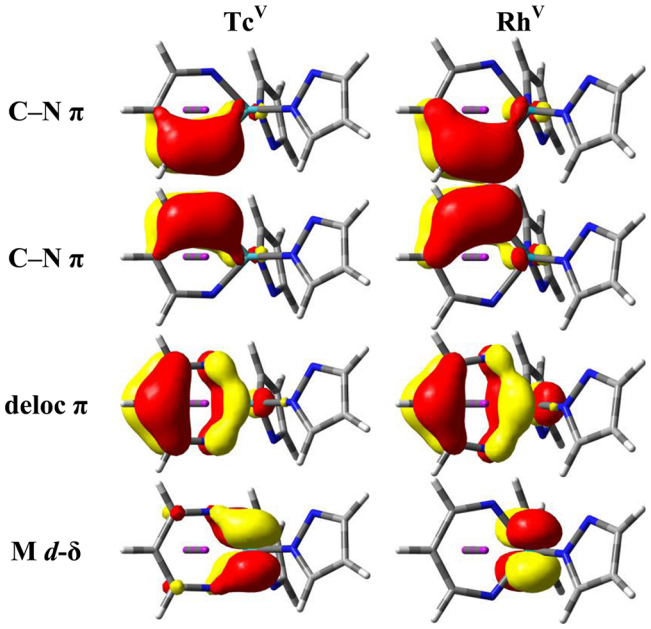

Figure 5. Molecular orbital isosurface plots (0.05 au) of the π orbitals for $[(pz)_2(Tc^V\text{-pyr})]^0$ and $[(pz)_2(Rh^V\text{-pyr})]^0$.

couples that will result in d^2 complexes with occupied $d-\delta$ and unoccupied $d-\pi$ orbitals that could afford metallapyrimidines with strong aromaticity.

CONCLUSIONS

In this paper, we have utilized the natural chemical shielding analysis to decompose $NICS(1)_{zz}$ contributions of metallapyrimidines into diamagnetic (field-free) and paramagnetic (field-induced) contributions from localized π orbitals for a new class of metallacycle, metallapyrimidines. $NICS(1)_{zz}$ for niobapyrimidine suggested that the ring is aromatic, but our NCS analysis showed this is not due to field-induced contributions. Instead, positive paramagnetic contributions suggest this species is better described as slightly antiaromatic instead of slightly aromatic, consistent with our finding of an isoenergetic isomer for this species that has a nonplanar niobapyrimidine ring. In a series of d^0 metallapyrimidines, all complexes demonstrated similar behavior, though the Tc^{VII} species was found to be nonaromatic, which prompted us to vary the d electron count of the metal. Variation of the metal d electron count was accomplished by studying a series of M^V metallapyrimidine complexes where M = Nb, Mo, Tc, Ru, and Rh, which span d^0 to d^4. These complexes were subjected to the NCS analysis, which showed strong evidence for aromaticity, with the negative $NICS(1)_{zz}$ values arising from large negative paramagnetic contributions in the $NICS(1)_{\pi zz}$.

One must always exercise caution when interpreting aromatic indicators of a single type as we have done here. However, the NCS data for the M^V complexes suggested to us a conceptual picture for how metallaaromaticity can be encouraged; both of the d orbitals capable of conjugating with the π system of kp^{3-} must be utilized. We discovered in the d^0 series that having both the $d-\pi$ and $d-\delta$ orbitals unoccupied, which can theoretically both act as acceptors, does not lead to aromaticity across a wide range of metal orbital energies that we accessed by varying the metal valency. Bond localization or nonplanarity was observed instead. Our M^V series of complexes showed that having one of these orbitals occupied and one unoccupied leads to clear examples of aromatic systems according to the NCS decomposition of the $NICS(1)_{zz}$ value. We suspect that the $d-\pi$ orbital must be unoccupied due to its ability to conjugate strongly with the ring π orbitals as an acceptor and provide a conduit for continuous electronic communication across the metallacycle, as evidenced by the large field-induced contribution from the deloc π orbital in the Tc^V and Rh^V species. The covalent character of this bonding is so persistent that the localization algorithm maintains delocalization of this orbital across the ring. The role of the $d-\delta$ orbital is less clear. We have interpreted it as conjugating with the ring here due to the nitrogen character in the deloc orbital plot for the Tc^V species, but its role may actually be to prevent certain structural distortions, as we observed for the d^0 complexes. If the latter is the case, then metallapyrimidines are classic 6 π electron systems,[28] though the distribution of electrons between the metal and ligand is different from that proposed for metallabenzene. Unfortunately, we encountered no examples of a doubly occupied $d-\pi$ and unoccupied $d-\delta$ orbital in our studies to verify this hypothesis explicitly. Alternative coordination environments are a promising avenue for exploration of this point in the future and may enable a unified theory for aromaticity in metallapyrimidines, and possibly metallacycles in general, as a function of not only the d electron count but the d orbital ordering. Future work will also include the evaluation of aromaticity in metallapyrimidines and related metallacycles using alternative aromaticity indicators, such as induced ring current measurements and computing barriers for cycloaddition chemistry at the metallapyrimidine.

ASSOCIATED CONTENT

Supporting Information

Full NCS orbital analysis, pictures of contributing π orbitals, optimized Cartesian coordinates, harmonic vibrational frequencies, SCF energies with ZPE, and thermal free energy corrections for all species in the study. This information is available free of charge via the Internet at http://pubs.acs.org.

AUTHOR INFORMATION

Corresponding Author

*E-mail: lordri@gvsu.edu.

Present Address

[†]Department of Chemistry, Grand Valley State University, Allendale, Michigan 49401

Notes

The authors declare no competing financial interest.

ACKNOWLEDGMENTS

Computational resources maintained by the Wayne State Grid are gratefully acknowledged. This research was funded by Grand Valley State University Start-Up funds (to R.L.L.) and U.S. National Science Foundation Grant Nos. CHE-1212281 (to H.B.S.), and CHE-0910475 and CHE-1212574 (to C.H.W.). B.T.P. and R.L.L. thank Drs. James Cheeseman, Hrant Hratchian, and Fernando Clemente at Gaussian Inc. for technical advice and assistance regarding the NCS calculations.

REFERENCES

(1) Hofmann, A. W. On insolinic acid. *Proc. R. Soc. London* **1856**, *8*, 1−3.

(2) Schleyer, P. v. R. Introduction: Aromaticity. *Chem. Rev.* **2001**, *101*, 1115−1118.

(3) Krygowski, T. M.; Cyrański, M. K. Structural aspects of aromaticity. *Chem. Rev.* **2001**, *101*, 1385−1420.
(4) Cyrański, M. K. Energetic aspects of cyclic π-electron delocalization: Evaluation of the methods of estimating aromatic stabilization energies. *Chem. Rev.* **2005**, *105*, 3773−3811.
(5) Schleyer, P. v. R. Introduction: Delocalization π and σ. *Chem. Rev.* **2005**, *105*, 3433−3435.
(6) Pople, J. A. Proton magnetic resonance of hydrocarbons. *J. Chem. Phys.* **1956**, *24*, 1111.
(7) (a) Viglione, R. G.; Zanasi, R.; Lazzeretti, P. Are ring currents still useful to rationalize the benzene proton magnetic shielding? *Org. Lett.* **2004**, *6*, 2265−2267. (b) Faglioni, F.; Ligabue, A.; Pelloni, S.; Soncini, A.; Viglione, R. G.; Ferraro, M. B.; Zanasi, R.; Lazzeretti, P. Why downfield proton chemical shifts are not reliable aromaticity indicators. *Org. Lett.* **2005**, *7*, 3457−3460. (c) Wannere, C. S.; Corminboeuf, C.; Allen, W. D.; Schaefer, H. F.; Schleyer, P. v. R. Downfield proton chemical shifts are not reliable aromaticity indicators. *Org. Lett.* **2005**, *7*, 1457−1460.
(8) (a) Gomes, J. A. N. F.; Mallion, R. B. Aromaticity and ring currents. *Chem. Rev.* **2001**, *101*, 1349−1384. (b) Chen, Z.; Wannere, C. S.; Corminboeuf, C.; Puchta, R.; Schleyer, P. v. R. Nucleus-independent chemical shifts (NICS) as an aromaticity criterion. *Chem. Rev.* **2005**, *105*, 3842−3888. (c) Geuenich, D.; Hess, K.; Köhler, F.; Herges, R. Anisotropy of the induced current density (ACID), a general method to quantify and visualize electronic delocalization. *Chem. Rev.* **2005**, *105*, 3758−3772. (d) Islas, R.; Heine, T.; Merino, G. The induced magnetic field. *Acc. Chem. Res.* **2011**, *45*, 215−228.
(9) (a) Bleeke, J. R. Metallabenzenes. *Chem. Rev.* **2001**, *101*, 1205−1228. (b) Wright, L. J. Metallabenzenes and metallabenzenoids. *Dalton Trans.* **2006**, 1821−1827.
(10) Thorn, D. L.; Hoffmann, R. Delocalization in metallocycles. *Nouv. J. Chim.* **1979**, *3*, 39−45.
(11) (a) Iron, M. A.; Lucassen, A. C. B.; Cohen, H.; van der Boom, M. E.; Martin, J. M. L. A computational foray into the formation and reactivity of metallabenzenes. *J. Am. Chem. Soc.* **2004**, *126*, 11699−11710. (b) Fernández, I.; Frenking, G. Aromaticity in Metallabenzenes. *Chem.—Eur. J.* **2007**, *13*, 5873−5884. (c) Periyasamy, G.; Burton, N. A.; Hillier, I. H.; Thomas, J. M. H. Electron delocalization in the metallabenzenes: A computational analysis of ring currents. *J. Phys. Chem. A* **2008**, *112*, 5960−5972. (d) Havenith, R. W. A.; De Proft, F.; Jenneskens, L. W.; Fowler, P. W. Relativistic ring currents in metallabenzenes: An analysis in terms of contributions of localized orbitals. *Phys. Chem. Chem. Phys.* **2012**, *14*, 9897−9905.
(12) Milčić, M. K.; Ostojić, B. D.; Zarić, S. D. Are chelate rings aromatic? Calculations of magnetic properties of acetylacetonato and o-benzoquinonediimine chelate rings. *Inorg. Chem.* **2007**, *46*, 7109−7114.
(13) Perera, T. H.; Lord, R. L.; Heeg, M. J.; Schlegel, H. B.; Winter, C. H. Metallapyrimidines and metallapyrimidiniums from oxidative addition of pyrazolate N−N bonds to niobium(III), niobium(IV), and tantalum(IV) metal centers and assessment of their aromatic character. *Organometallics* **2012**, *31*, 5971−5974.
(14) (a) Fallah-Bagher-Shaidaei, H.; Wannere, C. S.; Corminboeuf, C.; Puchta, R.; Schleyer, P. v. R. Which NICS aromaticity index for planar π rings is best? *Org. Lett.* **2006**, *8*, 863−866. (b) Schleyer, P. v. R.; Jiao, H.; Hommes, N. J. R. v. E.; Malkin, V. G.; Malkina, O. L. An evaluation of the aromaticity of inorganic rings: Refined evidence from magnetic properties. *J. Am. Chem. Soc.* **1997**, *119*, 12669−12670.
(15) Bohmann, J. A.; Weinhold, F.; Farrar, T. C. Natural chemical shielding analysis of nuclear magnetic resonance shielding tensors from gauge-including atomic orbital calculations. *J. Chem. Phys.* **1997**, *107*, 1173−1184.
(16) Frisch, M. J.; Trucks, G. W.; Schlegel, H. B.; Scuseria, G. E.; Robb, M. A.; Cheeseman, J. R.; Scalmani, G.; Barone, V.; Mennucci, B.; Petersson, G. A.; Nakatsuji, H.; Caricato, M.; Li, X.; Hratchian, H. P.; Izmaylov, A. F.; Bloino, J.; Zheng, G.; Sonnenberg, J. L.; Liang, W.; Hada, M.; Ehara, M.; Toyota, K.; Fukuda, R.; Hasegawa, J.; Ishida, M.; Nakajima, T.; Honda, Y.; Kitao, O.; Nakai, H.; Vreven, T.; Montgomery, J., J. A.; Peralta, J. E.; Ogliaro, F.; Bearpark, M.; Heyd, J. J.; Brothers, E.; Kudin, K. N.; Staroverov, V. N.; Keith, T.; Kobayashi, R.; Normand, J.; Raghavachari, K.; Rendell, A.; Burant, J. C.; Iyengar, S. S.; Tomasi, J.; Cossi, M.; Rega, N.; Millam, J. M.; Klene, M.; Knox, J. E.; Cross, J. B.; Bakken, V.; Adamo, C.; Jaramillo, J.; Gomperts, R.; Stratmann, R. E.; Yazyev, O.; Austin, A. J.; Cammi, R.; Pomelli, C.; Ochterski, J. W.; Martin, J. M. L.; Morokuma, K.; Zakrzewski, V. G.; Voth, G. A.; Salvador, P.; Dannenberg, J. J.; Dapprich, S.; Parandekar, P. V.; Mayhall, N. J.; Daniels, A. D.; Farkas, O.; Foresman, J. B.; Ortiz, J. V.; Cioslowski, J.; Fox, D. J. *Gaussian Development Version, Revision H.20+*; Gaussian, Inc.: Wallingford, CT, 2010.
(17) (a) Vosko, S. H.; Wilk, L.; Nusair, M. Accurate spin-dependent electron liquid correlation energies for local spin density calculations: A critical analysis. *Can. J. Phys.* **1980**, *58*, 1200−1211. (b) Lee, C.; Yang, W.; Parr, R. G. Development of the Colle−Salvetti correlation-energy formula into a functional of the electron density. *Phys. Rev. B* **1988**, *37*, 785. (c) Becke, A. D. Density functional thermochemistry. III. The role of exact exchange. *J. Chem. Phys.* **1993**, *98*, 5648. (d) Stephens, P. J.; Devlin, F. J.; Chabalowski, C. F.; Frisch, M. J. Ab initio calculation of vibrational absorption and circular dichroism spectra using density functional force fields. *J. Phys. Chem.* **1994**, *98*, 11623−11627.
(18) (a) Kaupp, M.; Schleyer, P. V.; Stoll, H.; Preuss, H. Pseudopotential approaches to Ca, Sr, and Ba hydrides—Why are some alkaline-earth Mx2 compounds bent? *J. Chem. Phys.* **1991**, *94*, 1360−1366. (b) Bergner, A.; Dolg, M.; Kuchle, W.; Stoll, H.; Preuss, H. Ab-initio energy-adjusted pseudopotentials for elements of groups 13−17. *Mol. Phys.* **1993**, *80*, 1431−1441. (c) Dolg, M.; Stoll, H.; Preuss, H.; Pitzer, R. M. Relativistic and correlation-effects for element 105 (Hahnium, Ha)—A comparative-study of M and Mo (M = Nb, Ta, Ha) using energy-adjusted ab initio pseudopotentials. *J. Phys. Chem.* **1993**, *97*, 5852−5859.
(19) (a) Schlegel, H. B.; McDouall, J. J. In *Computational Advances in Organic Chemistry*; Ögretir, C., Csizmadia, I. G., Eds.; Kluwer Academic: Amsterdam, 1991; (b) Bauernschmitt, R.; Ahlrichs, R. Stability analysis for solutions of the closed shell Kohn−Sham equation. *J. Chem. Phys.* **1996**, *104*, 9047.
(20) Schlegel, H. B. Optimization of equilibrium geometries and transition structures. *J. Comput. Chem.* **1982**, *3*, 214−18.
(21) Fukui, K. The path of chemical reactions—The IRC approach. *Acc. Chem. Res.* **1981**, *14*, 363−368.
(22) Foresman, J. B.; Frisch, A. *Exploring Chemistry with Electronic Structure Methods*, 2nd ed.; Gaussian, Inc.: Wallingford, CT, 1996.
(23) Schleyer, P. v. R.; Maerker, C.; Dransfeld, A.; Jiao, H.; Hommes, N. J. R. v. E. Nucleus-independent chemical shifts: A simple and efficient aromaticity probe. *J. Am. Chem. Soc.* **1996**, *118*, 6317−6318.
(24) Cheeseman, J. R.; Trucks, G. W.; Keith, T. A.; Frisch, M. J. A comparison of models for calculating nuclear magnetic resonance shielding tensors. *J. Chem. Phys.* **1996**, *104*, 5497−5509.
(25) Glendening, E. D.; Reed, A. E.; Carpenter, J. E.; Weinhold, F. *NBO Version 3.1*; Gaussian, Inc.: Wallingford, CT, 2009.
(26) Dezelah; Wiedmann, M. K.; Mizohata, K.; Baird, R. J.; Niinistö, L.; Winter, C. H. A Pyrazolate-based metalorganic tantalum precursor that exhibits high thermal stability and its use in the atomic layer deposition of Ta_2O_5. *J. Am. Chem. Soc.* **2007**, *129*, 12370−12371.
(27) Rinehart, J. D.; Kozimor, S. A.; Long, J. R. Tetranuclear uranium clusters by reductive cleavage of 3,5-dimethylpyrazolate. *Angew. Chem., Int. Ed.* **2010**, *49*, 2560−2564.
(28) We analyzed the Tc(V) and Rh(V) metallapyrimidine complexes including the contributions of the *d*−δ orbital, but all conclusions are qualitatively the same if we only consider the 6 π electrons.